

RESONANCE BROADENING OF THE SODIUM D LINES

John Huennekens and Alan Gallagher*

Joint Institute for Laboratory Astrophysics, University of Colorado and
National Bureau of Standards, Boulder, CO 80309

Abstract

Sodium vapor, in the density range 10^{13} – 5×10^{14} cm^{-3} , was excited by a cw dye laser, tuned 20–140 GHz from either the D_1 or D_2 resonance line. We observed the three peak scattered spectrum, consisting of the Rayleigh component at the laser frequency, and the two fluorescence components (direct and sensitized) at the atomic resonance-line frequencies. Corrections to the Rayleigh signals for anisotropy and polarization effects, and to the fluorescence signals for radiation trapping effects were made in order to obtain the ratio of the intensity of the fluorescence components to that of the Rayleigh component. This ratio of fluorescence to Rayleigh intensity combined with a measurement of the line-wing absorption coefficient yields the sodium density and the D-line self-broadening rate coefficients ($k_{Br2} = 4.67 \times 10^{-7} \text{ cm}^3 \text{ s}^{-1} \pm 15\%$ for the D_2 line and $k_{Br1} = 3.07 \times 10^{-7} \text{ cm}^3 \text{ s}^{-1} \pm 15\%$ for the D_1 line). Asymmetry in the self-broadened line wings due to fine structure recoupling was observed. Asymmetry in the Rayleigh scattering, as a function of detuning, was also observed, due to interference between the two fine structure levels. In addition, the measured intensity ratio of the D-lines combined with pulsed measurements of the effective radiative decay rate in the presence of radiation trapping yields the fine structure collisional mixing cross section ($\sigma_{3P_{3/2} \rightarrow 3P_{1/2}} = 172 \text{ \AA}^2 \pm 18\%$). Our results are compared to other experiments and to theory.

*Staff Member, Quantum Physics Division, National Bureau of Standards.

Since Holtzmark's [1] pioneering work, the theory of resonance broadening in the impact regime has steadily progressed, until at present, good agreement between experiment and theory exists for $J = 0$ to $J = 1$ transitions [2]. Ali and Griem [3] and Carrington, Stacey and Cooper [4] have extended the calculations to include $J = 1/2$ to $J = 1/2$ and $J = 1/2$ to $J = 3/2$ transitions appropriate for the alkalis, but so far there are not many data on these systems. The available data have rather large uncertainties, typically 40%, due primarily to uncertainties in vapor pressure, and the data barely agree with theory within those uncertainties. Our aim in the present experiment was to provide a more accurate test of theory by independently measuring both the absorption coefficient and the ratio of the line-broadening and natural decay rates. This ratio is obtained from the ratio of redistributed fluorescence to Rayleigh scattering when the laser is tuned into the line wings.

Figure 1 is a block diagram of the experimental apparatus, which is described fully in Ref. [5]. The cell is a stainless steel block drilled out to make a cross and vacuum sealed to sapphire windows with metal O rings. Only the vapor-containing cross is depicted in the figure. Two arms of the cross contain sapphire rods (indicated by cross hatching in the figure) which serve to reduce optical depth in those directions, and to create a geometry which simplifies radiation trapping calculations required for the interpretation of the results. The cell contains sodium in the density range 1×10^{13} – 5×10^{14} cm^{-3} with no buffer gas. The density is controlled by the temperature of the side arm which is kept 25–50°C below the cell and window temperature to prevent condensation on the windows. The laser is a single mode cw dye laser. Fluorescence is monitored at right angles to the laser beam with a 3/4 meter double monochromator and a photomultiplier with an S-20 cathode response. The PMT output is sent to an electrometer, divided by laser power, and finally displayed on a chart recorder. PMT 2 in the figure is used to obtain absorption scans.

We detune the laser, typically 20–140 GHz from either the D_1 or D_2 resonance line, and observe the three-peaked scattered spectrum consisting

Fig. 1. Block diagram of the experimental apparatus.

of the Rayleigh components at the center and wings. Fig. 2a shows the relative intensities of the excitation components due to collisions with ground state atoms, collisional transfer to other levels respectively, and the Rayleigh lines, respectively. The coherent superposition of the two terms are in general out of phase where τ_c is the collisional lifetime constant, Γ_{Br2} is the desired impact rate thought of as the limit, $\Gamma_{Br1}(\Delta_1)$ the densities u

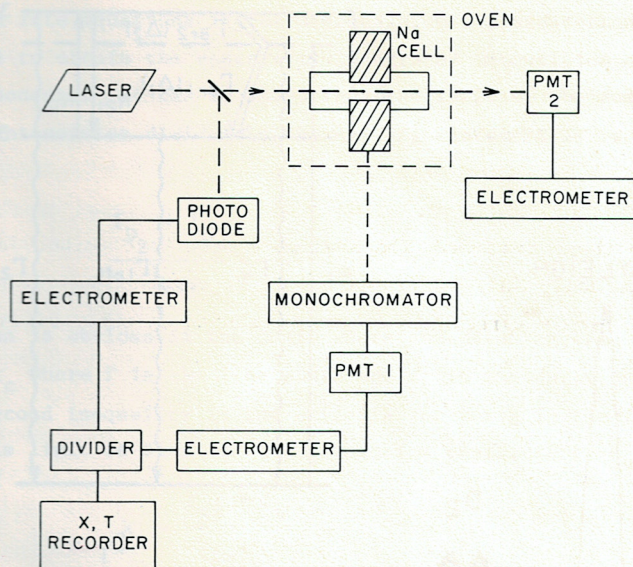


Fig. 1. Block diagram of the experimental setup. Sapphire rods inside the cell are indicated by cross hatching. PMT = photomultiplier.

of the Rayleigh peak at the laser frequency, and the two fluorescence components at the two atomic resonance frequencies (see Fig. 2b). Figure 2a shows the relevant collisional and radiative rates. R_{21} and R_{12} are the excitation transfer rates between the $3P_{3/2}$ and $3P_{1/2}$ levels due to collisions with ground state atoms. $\Gamma_{Br1}(\Delta_1)$ and $\Gamma_{Br2}(\Delta_2)$ are the total collisional transfer rates from the virtual level to the $3P_{1/2}$ and $3P_{3/2}$ levels respectively. Here Δ_1 and Δ_2 are the detunings from the D_1 and D_2 lines, respectively. Since the virtual level can be characterized as a coherent superposition of the ground state and both excited states, these terms are in general quite complicated. However, for $\Delta_2 \ll 1/\tau_c \ll \Delta_1$ where τ_c is the duration of a collision, the term $\Gamma_{Br2}(\Delta_2)$ reduces to a constant, $\Gamma_{Br2} \equiv nk_{Br2}$ (where n is the sodium density), which is the desired impact regime self-broadened width of the D_2 line. (Γ_{Br2} can also be thought of as the collisional rate of destruction of coherence.) In this limit, $\Gamma_{Br1}(\Delta_1)$ approaches the inelastic rate, R_{21} , and can be ignored at the densities used here since radiation trapping causes this term to be a

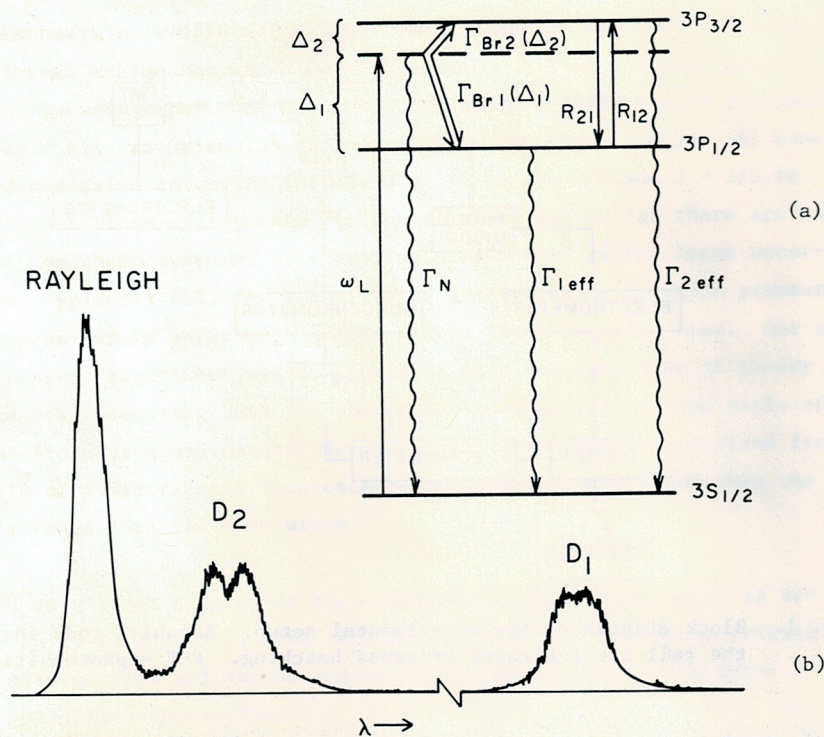


Fig. 2. a) Relevant collisional and radiative rates in sodium excited off resonance by a narrow band cw laser. Symbols are explained in text.
 b) Three peak scattered spectrum. Laser was detuned 31.1 GHz to the red of D_2 . Na density = $1.51 \times 10^{14} \text{ cm}^{-3}$.

negligible source of $3P_{1/2}$ population compared to the $3P_{3/2} \rightarrow 3P_{1/2}$ excitation transfer process. Similarly, for $\Delta_1 \ll 1/\tau_c \ll \Delta_2$ the term $\Gamma_{Br1}(\Delta_1)$ reduces to a constant, $\Gamma_{Br1} \equiv nk_{Br1}$, and $\Gamma_{Br2}(\Delta_2)$ tends toward R_{12} and can also be ignored [6]. The other Γ 's in Fig. 2a are radiative rates. It is important to note that while the off-resonant Rayleigh scattering is characterized by the natural radiative rate, Γ_N , the two fluorescence components must be described by the much slower effective rates Γ_{1eff} and Γ_{2eff} due to radiation trapping at the high optical depths of this experiment. Radiation trapping is also responsible for the self reversal apparent on the D_2 component in Fig. 2b and just barely visible on the D_1 component.

We have solved rate equations in the dressed atom representation (see Refs. [5,7,8]) to obtain the spectrally integrated intensities of each of the three components. It can be shown that the ratio of the sum of the fluorescence intensities divided by the Rayleigh intensities is equal to Γ_{Br}/Γ_N , i.e.

$$\frac{I_{D2} + I_{D1}}{I_{Ray}} = \frac{\Gamma_{Br}}{\Gamma_N} \quad (1)$$

This expression is obvious in the limit where the detuning, $\Delta\omega$, satisfies $\Gamma \ll \Delta\omega \ll 1/\tau_c$ where Γ is the line width and τ_c is the duration of a collision (the second inequality is the criteria for being in the impact regime). In this limit we find for the absorption coefficient, k_v :

$$k_v \propto \frac{\Gamma_{Br} + \Gamma_N}{(\Delta\omega)^2} \quad (2)$$

The term proportional to Γ_N gives rise to the Rayleigh scattering or non-redistributed light at the laser frequency, while the term proportional to Γ_{Br} gives rise to the collisionally redistributed light at the two atomic resonance frequencies. Thus Eq. (1) follows automatically in this limit.

There are several advantages to measuring resonance broadening by this technique. First we measure both the fluorescence to Rayleigh ratio and the absorption coefficient, k_v . From these two pieces of information we can obtain both Γ_{Br} and the Na density, thus eliminating the major source of uncertainty in pure absorption measurements in which the density is typically obtained from a vapor pressure vs. temperature relationship. However, densities we have obtained in this manner differ from Nesmeyanov's [9] relationship by less than 15%. Secondly, we can measure the broadening rate even when $\Gamma_{Br} < \Gamma_N$ which is difficult to do in a pure absorption measurement.

The intensities appearing in Eq. (1) are the spectrally integrated intensities averaged over angle. We do not, however, detect light over the entire 4π solid angle, but instead over a small solid angle $d\Omega$. Since both the fluorescence and Rayleigh components emerge from the cell

anisotropically, Eq. (1) must be modified to include such effects. The Rayleigh scattering is anisotropic due to use of an anisotropic and linearly polarized source and can be easily calculated from well-known Rayleigh scattering angular distributions [5,10]. The fluorescence is anisotropic as it emerges from the cell, due to radiation trapping and the particular cell geometry. We are working at optical depths in the range $k_0\lambda \approx 100-1000$ and we can use Holstein's [11] theory of radiation trapping to calculate escape probabilities and therefore the fluorescence anisotropy. Details of these calculations may be found in Refs. [5] and [12].

We observe the fluorescence to Rayleigh ratio for several detunings near both the D_1 and D_2 lines. Figure 3 shows $I_{\text{Ray}}/(I_{D_2}+I_{D_1})$ as a function of detuning from both lines at $[\text{Na}] = 1.97 \times 10^{14} \text{ cm}^{-3}$. It is apparent that in both cases, the ratio is asymmetric as a function of detuning. This occurs since both the Rayleigh signal and the fluorescence signals are asymmetric for reasons that will be explained shortly. To obtain the impact

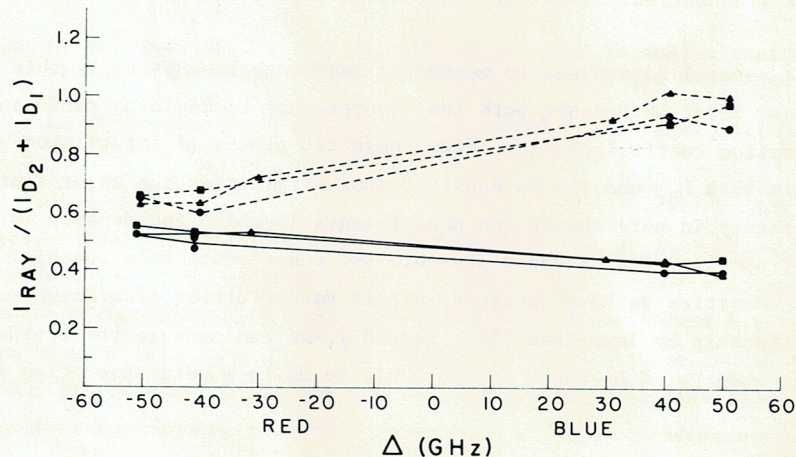


Fig. 3. Measured ratio of the integrated Rayleigh intensity to the sum of the two fluorescence component intensities. Detunings are with respect to the D_1 and D_2 line centroids. Different symbols represent different data runs. Solid lines are pumping D_2 , dashed lines are pumping D_1 . $[\text{Na}] = 1.97 \times 10^{14} \text{ cm}^{-3}$.

limit on Γ_{Br} , dating which takes i effects.

Figure 4 is a plo The expected line we have obtained along with the re [14]. The system and Pichler appear termination but t Our results are i tions, which are however, small en Ali and Griem res

From the fluores collisional part

Fig. 4. Γ_{Br} vs. are Γ_{Br}

limit on Γ_{Br} , data such as those in Fig. 3 are interpolated to zero detuning which takes into account at least first-order corrections for these effects.

Figure 4 is a plot of measured values of Γ_{Br} as a function of Na density. The expected linear dependence is evident. The results for $k_{Br} \equiv \Gamma_{Br}/n$ we have obtained from data such as those in Fig. 4 are listed in Table 1 along with the results of Niemax and Pichler [13] and those of Watanabe [14]. The systematic discrepancy between our results and those of Niemax and Pichler appears to be due to a systematic effect in their density determination but this difference falls within their estimated uncertainty. Our results are in very good agreement with the Carrington *et al.* calculations, which are also given in the table. Our $\pm 15\%$ uncertainties are not, however, small enough to distinguish between the Carrington *et al.* and the Ali and Griem results.

From the fluorescence intensity as a function of detuning we obtain the collisional part of the absorption coefficient, defined as $\Gamma_{Br}(\Delta\nu)/(\Delta\nu)^2$

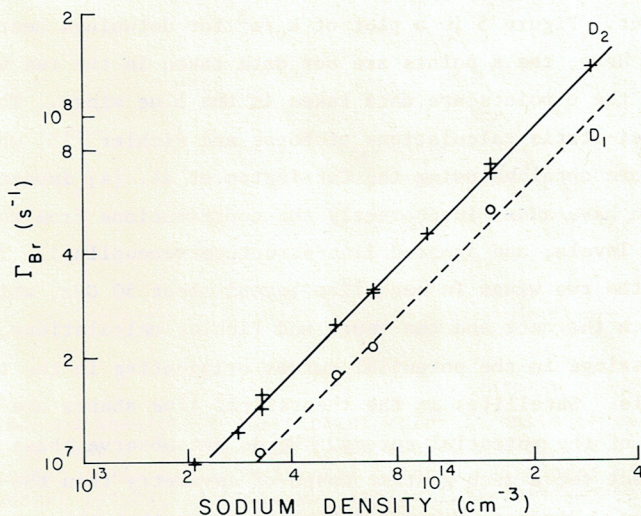


Fig. 4. Γ_{Br} vs. [Na]. Dashed curve and o's are Γ_{Br1} , solid curve and +'s are Γ_{Br2} .

Table 1
Comparison of Experimental and Theoretical Determinations
of the Sodium Resonance Broadening Parameters, k_{Br2}
for the D_2 Line and k_{Br1} for the D_1 Line

Author	k_{Br2} (cm^3/s)	k_{Br1} (cm^3/s)	k_{Br2}/k_{Br1}
Experimental			
This work	$4.67 \times 10^{-7} \pm 15\%$	$3.07 \times 10^{-7} \pm 15\%$	$1.52 \pm 10\%$
Niemax and Pichler [13]	$6.84 \times 10^{-7} \pm 30-50\%$	$5.79 \times 10^{-7} \pm 30-50\%$	$1.18 \pm 30-50\%$
Watanabe [14]	$5.85 \times 10^{-7} \pm 20\%$	$5.04 \times 10^{-7} \pm 20\%$	1.16
Theoretical			
Carrington et al. [4]	4.79×10^{-7} a	2.94×10^{-7} b	1.63
Ali and Griem [3]	4.42×10^{-7} c	3.13×10^{-7} c	1.41

$${}^a k_{Br2} = 2\pi \times 1.47 e^{2f/m\omega}.$$

$${}^b k_{Br1} = 2\pi \times 1.805 e^{2f/m\omega}.$$

$${}^c k_{Br} = 2\pi \times 1.92 (g_1/g_2)^{1/2} e^{2f/m\omega}.$$

times a constant. Figure 5 is a plot of k_v/n^2 for detunings near the D_1 and D_2 lines. Here, the x points are our data taken in the red wing of each line, and the o points are data taken in the blue wings. The solid curves are quasi-static calculations of Movre and Pichler [15] while the dashed curves are obtained using the Carrington et al. [4] impact regime Γ_{Br} 's (where we have added incoherently the contributions from the two fine-structure levels, and ignored fine-structure recoupling). The asymmetry between the two wings in each line beyond about 50 GHz, which is apparent in both the data and the Movre and Pichler calculations, is due to avoided crossings in the potential curves originating in the two fine structure levels. Satellites in the theoretical line shapes are due to extrema in two of the potential curves. We do not observe these satellites and in fact see a much gentler onset of asymmetry than the calculation indicates. However, Movre and Pichler argue that the satellites should be severely washed out in the lighter alkalis such as sodium due to a breakdown in the quasi-static approximation at the satellite detunings.

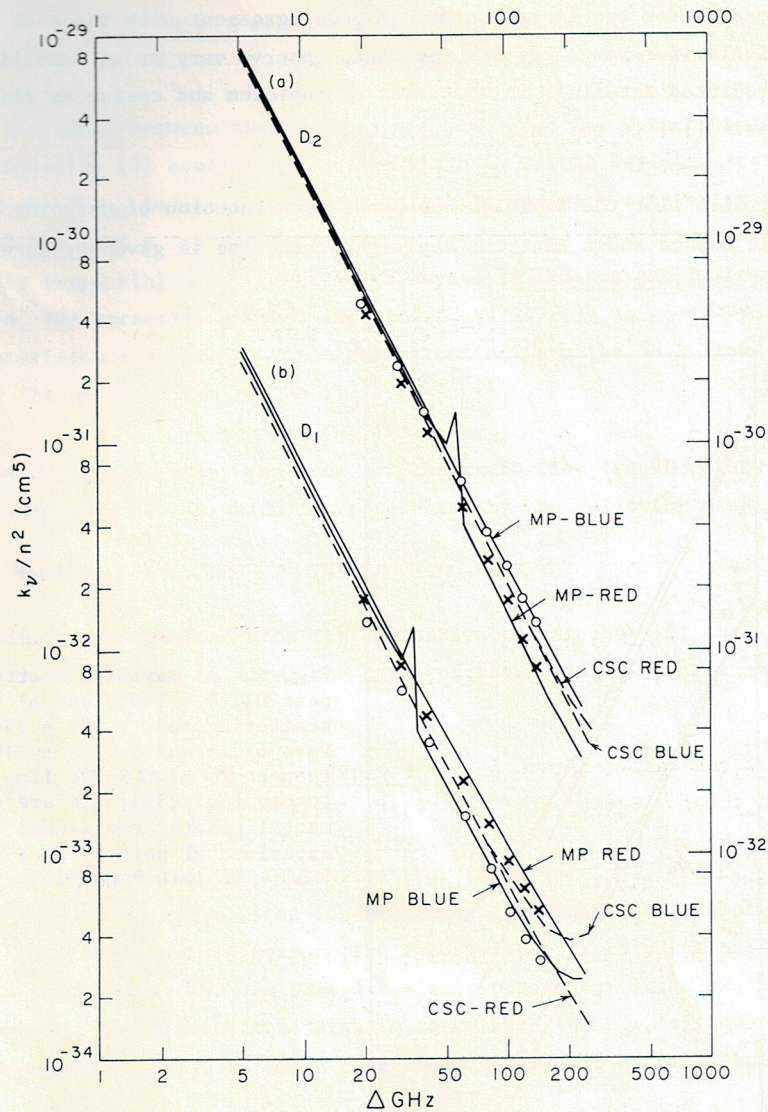


Fig. 5. Reduced absorption coefficient k_v/n^2 in units of cm^5 for detunings near a) the D_2 line (left scale) and b) the D_1 line (right scale). 'x's are experimental points, red wings; 'o's are experimental points, blue wings. $[\text{Na}] = 1.51 \times 10^{14} \text{ cm}^{-3}$. Solid lines are a quasi-static calculation of Movre and Pichler (Ref. [15]). Dashed lines are obtained from the impact regime Γ_{Br} 's calculated by Carrington *et al.* (Ref. [4]) where we have added incoherently the contributions of the two fine structure levels ignoring fine structure recoupling.

Our results for the lineshape are in good agreement with those of Niemax and Pichler for Na. They did, in fact, observe very broad satellites at the predicted detunings in the cases of rubidium and cesium as did Awan and Lewis [16] in the case of rubidium.

We may also plot the Rayleigh component as a function of detuning (Fig. 6). It can be shown that the Rayleigh scattering is given by an expression of the form [5]:

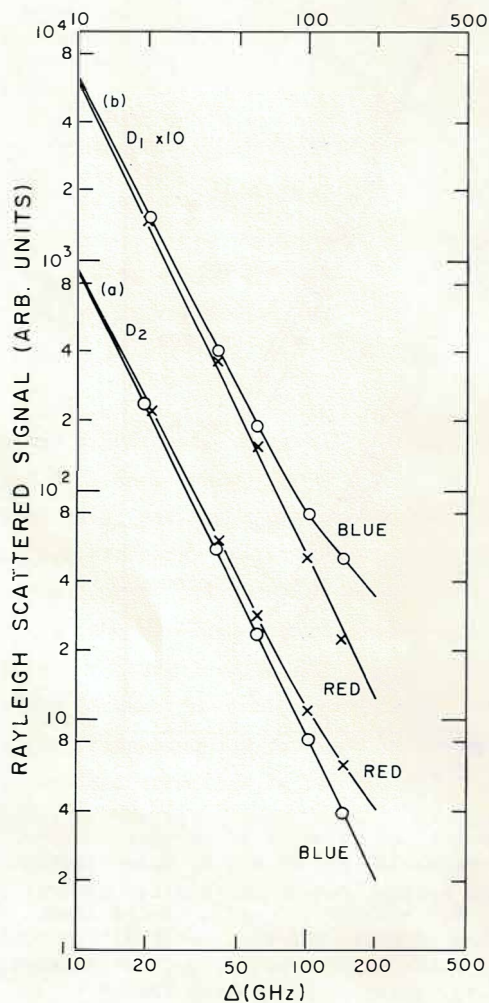


Fig. 6. a) Rayleigh scattering near D_2 , $\theta = 146^\circ$, and b) Rayleigh scattering near D_1 , $\theta = 146^\circ$. Part b) is multiplied by 10 with respect to a). Solid line is theory [Eq. (3)]; x's are experimental points, red wings; o's are experimental points, blue wings. $[Na] = 1.51 \times 10^{14} \text{ cm}^{-3}$.

Here θ is the
direction. Equ
tering off th
the $3P_{3/2}$ lev
is primarily
from Fig. 6,
type of inter
previously di

Finally, we
the $3P_{3/2}$ and

Na

Again workin
the laser tu
is given by:

where E_{21} an
are the effe
(see Fig. 2a
resonant cw
and time-res
[5]). The r

Our results
are shown in
The experim
vironment us
were made of
tion of dist

$$I_{\text{Ray}} = \frac{2}{\Delta_1^2} + \frac{2 + 3 \sin^2 \theta}{\Delta_2^2} + \frac{6 \sin^2 \theta - 4}{\Delta_1 \Delta_2} \quad (3)$$

Here θ is the angle between the laser polarization and the detection direction. Equation (3) consists of a term which is simple Rayleigh scattering off the $3P_{1/2}$ level, a term that is simple Rayleigh scattering off the $3P_{3/2}$ level, and a quantum interference term. This interference term is primarily responsible for the Rayleigh asymmetry and, as can be seen from Fig. 6, the agreement between experiment and Eq. (3) is good. This type of interference effect in Rayleigh scattering near the Na D lines was previously discussed by Tam and Au [17].

Finally, we can obtain cross sections for the excitation transfer between the $3P_{3/2}$ and $3P_{1/2}$ levels which is represented by the following equation

$$\text{Na}(3P_{3/2}) + \text{Na}(3S) \xrightarrow{\quad} \text{Na}(3P_{1/2}) + \text{Na}(3S) \quad (4)$$

Again working in the dressed-atom representation we can show [5] that for the laser tuned near the D_2 line, the ratio of the D_1 to D_2 fluorescence is given by:

$$\frac{I_{D_1}}{I_{D_2}} = \frac{R_{21}}{\Gamma_{2\text{eff}}} \frac{\Gamma_{1\text{eff}}}{(\Gamma_{1\text{eff}} + R_{12})} \quad (5)$$

where R_{21} and R_{12} are the excitation transfer rates and $\Gamma_{1\text{eff}}$ and $\Gamma_{2\text{eff}}$ are the effective radiative rates in the presence of radiation trapping (see Fig. 2a). We therefore measure the fluorescence ratio using the off-resonant cw excitation. We use pulsed N_2 -laser pumped dye laser excitation and time-resolve the fluorescence signals to measure the Γ_{eff} 's (see Ref. [5]). The ratio, R_{12}/R_{21} , is taken from the principle of detailed balance.

Our results for the cross sections for the processes described by Eq. (4) are shown in Table 2. They are compared to two previous measurements. The experiment of Seiwert [18] was carried out in an optically thick environment using a resonance lamp excitation source. Detailed calculations were made of the excitation intensity and spectral distribution as a function of distance into the vapor, and similar calculations for the exiting

Table 2
Experimental and Theoretical Cross Sections
for Excitation Transfer in Na-Na Collisions

Authors	σ_{21}^a (\AA^2)	σ_{12}^b (\AA^2)	Temp (K)
	Experiment		
This work	172±18%	330±18%	575
Pitre and Krause [19]	283	532	424
Seiwert [18]	100	170	560
	Theory		
Dashevskaya <u>et al.</u> [20]	101		
Vdovin <u>et al.</u> [21]	131	229	

$^a\sigma_{21}$ is the cross section for
 $\text{Na}(3S) + \text{Na}(3P_{3/2}) \rightarrow \text{Na}(3S) + \text{Na}(3P_{1/2})$.

$^b\sigma_{12}$ is the cross section for
 $\text{Na}(3S) + \text{Na}(3P_{1/2}) \rightarrow \text{Na}(3S) + \text{Na}(3P_{3/2})$.

fluorescence were also made. These calculations are quite difficult and the level of agreement between Seiwert's results and the other two experiments is somewhat remarkable. Pitre and Krause [19] worked at low optical depth which in many ways is the right way to do the experiment since radiation trapping effects do not exist, and the fluorescence ratio (5) simply reduces to R_{21}/Γ_N . However, they took the density from a vapor pressure curve which can lead to large uncertainties whereas we had a direct measure of the density as stated earlier. Also they were working with fluorescence ratios on the order of 10^{-6} which necessitates great care in calibrating everything; particularly neutral density filters.

In Table 2 we also list two theoretical determinations of the excitation transfer cross sections. These are not terribly far from what we measured, but, similar calculations in other alkalis have produced results

that differ from experiment by as much as an order of magnitude, and we therefore do not attach much significance to this level of agreement. It is hoped that these new experimental results will encourage new calculations of this cross section using the improved potential curves of Movre and Pichler.

Acknowledgments

We would like to thank Drs. Jinx Cooper and Keith Burnett for many enlightening discussions during the course of this work. We would also like to thank Dr. Wolfgang Kamke for much assistance with operation of the laser. This research was supported in part by National Science Foundation grant PHY79-04928 through the University of Colorado.

References

1. J. Holtsmark: *Z. Physik* 34, 722 (1925).
2. E. L. Lewis: *Phys. Rep.* 58, #1 (1980).
3. A. W. Ali and H. R. Griem: *Phys. Rev.* 140, A1044 (1965); 144, A366 (1966).
4. C. G. Carrington, D. N. Stacey and J. Cooper: *J. Phys. B* 6, 417 (1973).
5. J. P. Huennekens: Ph.D. Thesis, University of Colorado (1982).
6. We would like to thank David Pritchard and Derek Robb for useful discussions concerning these terms. See also David Pritchard's article in this volume for further discussion.
7. S. Reynaud and C. Cohen-Tannoudji: "Collision effects in resonance fluorescence," in *Laser Spectroscopy V*, ed. by A. R. W. McKellar, T. Oka and B. P. Stoicheff (Springer-Verlag, Berlin, 1981), p. 166.
8. K. Burnett, J. Cooper, P. D. Kleiber and A. Ben-Reuven: *Phys. Rev. A* 25, 1345 (1982).
9. A. N. Nesmayanov: *Vapor Pressure of the Elements* (Academic, New York, 1963).
10. R. J. Ballagh and J. Cooper: *Astrophys. J.* 213, 479 (1977).
11. T. Holstein: *Phys. Rev.* 72, 1212 (1947); 83, 1159 (1951).

12. J. P. Huennekens and A. C. Gallagher: "Self broadening of the sodium resonance lines and excitation transfer between the $3P_{3/2}$ and $3P_{1/2}$ levels," manuscript in preparation.
13. K. Niemax and G. Pichler: J. Phys. B 8, 179 (1975).
14. K. Watanabe: Phys. Rev. 59, 151 (1941).
15. M. Movre and G. Pichler: J. Phys. B 10, 2631 (1977); 13, 697 (1980).
16. M. S. Awan and E. L. Lewis: J. Phys. B 9, L551 (1976).
17. A. C. Tam and C. K. Au: Opt. Comm. 19, 265 (1976).
18. R. Seiwert: Ann. Physik 18, 54 (1956).
19. J. Pitre and L. Krause: Can. J. Phys. 46, 125 (1968).
20. E. I. Dashevskaya, A. I. Voronin and E. E. Nikitin: Can. J. Phys. 47, 1237 (1969).
21. Yu. A. Vdovin, V. M. Galitskii and N. A. Dobrodeev: Sov. Phys.-JETP 29, 722 (1969).